Investigation of Cure and Nanomechanical Properties of Weatherable UV-cured Hardcoats

Jennifer David, Momentive Performance Materials, Waterford, NY, USA
Christoph Hilgers, Momentive Performance Materials, Leverkusen, Germany
Andreas Haeuseler, Momentive Performance Materials, Leverkusen, Germany
Karsten Moeller, University of Applied Science Niederrhein, Krefeld, Germany

Abstract

The majority of automotive polycarbonate headlamp lenses are coated with UV-curable coatings in order to improve weathering performance as well as abrasion and chemical resistance to fulfill SAE/FMVSS requirements. In this study the use of different UV-lamps and their impact on physical properties of 3-5 year weatherable coatings for automotive headlamps is summarized. Double bond conversion was measured by FTIR-ATR, and nanomechanical properties were tested and correlated with cure and typical physical property measures.

Introduction

The three lamps used in this study were all commercially available mercury lamps. One was a standard mercury lamp (Hg), one was doped with iron (Fe) and one was doped with gallium (Ga). The presence of the dopants results in a shift in the spectrum of light generated by the lamps such that the relative levels of UV-A, UV-B and UV-C light are different for each. These differences can affect the relative levels of surface cure compared to through-section cure. For example, the choice of a Ga-type lamp, which produces a relatively high level of UV-A, is often desirable for curing thick or heavily pigmented coatings compared with a standard Hg-type lamp. It was of interest to examine these three lamps to determine whether there would be a measurable difference in cure level for a clear 10 micron thick automotive coating.

Other researchers have used cross-section nanoindentation successfully to compare the mechanical property changes in coatings with the chemical changes as measured by other techniques. Some have studied the effects of photodegradation as a function of depth.[1,2] Additionally, the effects of processing changes as a function of depth have been examined.[3,4] In this study, nanomechanical testing is used to assess the implications of the level of double bond conversion on the physical properties, stiffness and abrasion resistance, of the resultant coatings. Physical measurements at the top surfaces of the samples were correlated directly with the FTIR-ATR spectroscopy measurements on these same top surfaces. Additionally, by preparing cross-sections these same physical properties of the coatings were measured as a function of depth.

Experimental Methods

Sample Preparation

Three different coating formulations were studied in this evaluation: a standard three year weatherable coating (3YR-STD), a modified version of this coating that can achieve higher double-bond conversion at the same energy dose level (3YR-MOD), and a standard five year weatherable coating (5YR-STD). Samples subjected to FTIR-ATR analysis were prepared on glass panels (3" x 3") by flow coating. Samples used in nanomechanical and other physical property testing were prepared on polycarbonate panels (4" x 9.75") by flow coating. After each coating was applied, a 6 min flash period at 75 °C was followed by UV cure at ambient conditions. For each of the UV-lamp cure conditions utilized in this study, the glass panels and the polycarbonate panels were cured together so that the properties of the coatings at each cure condition would be as comparable as possible. Three different UV-lamps (Hg, Fe, and Ga) were utilized at four different levels of cure energy (500, 1,000, 2,000, 3,000 and 4,000 mJ) at 200-250 mW/cm^2 UVA range (320-390 nm). The UV energy was measured with a UV Power Puck† II from EIT†.). Coating thicknesses were measured with a Filmetrics F20 using optical interferometry.

FTIR-ATR Analysis

A Thermo Nicolet† 6700 FTIR Spectrometer was used in attenuated total reflectance mode to collect the FTIR-ATR spectra. Acquisition was done in 64 scans from 4,000 cm^{-1} to 650 cm^{-1} at 4 cm^{-1} resolution with no ATR correction. A single bounce, 45° angle, Smart Orbit† diamond ATR crystal was used to perform the measurements along with a MCT-A detector. The band used to monitor cure was the C=C-H out of plane deformation at around 808 cm^{-1} and the area of this band was normalized to the area of the carbonyl band at 1,720 cm^{-1}. Spectra of uncured coatings were used as the 0% cure measurement.

The "Top" scans were obtained from the top surface of the coating as it was prepared on the glass panel. The "Bottom" scans were obtained by removing the coating from the glass panel using a piece of reinforced tape and then testing the side of the coating that had been in contact with the glass. The calculated percent cure values were reported as the average measured at three locations on each glass panel for a given coating-lamp combination. All FTIR-ATR testing for a given coating type was performed at locations with the same coating thicknesses to ensure that top and bottom surface results would be directly comparable for a given coating regardless of lamp type used during cure.

Nanomechanical Analysis

All nanomechanical testing was performed using a Hysitron TI 950 TriboIndenter† with a DMA transducer and a Berkovich probe. Testing was done on the coatings prepared on the plastic panels. Quasi-static "Top" measurements were made in displacement control mode on the coating surface as it was prepared. The load profile used was a five second load, a five second hold, and a one second un-load. This testing was performed at penetration depths which corresponded to contact depths of 5.0% ± 0.1% of the topcoat thickness. About 15 indents were performed in either two or three locations for each sample with 10 micron spacing (30-45 indents total). Outlier curves were removed and average data for modulus (E_r) and hardness (H) were computed. Modulus is a measure of the stiffness of a

material, the amount of force needed to elastically deform the material. Hardness is a measure of the material's resistance to plastic deformation. The hardness-to-modulus ratio (H/E_r) as described by Leyland and Matthews in 2000, was reported by a number of researchers in subsequent works to predict abrasion resistance in performance wear tests.[5] Past work in this laboratory has confirmed a strong correlation between both the hardness and the hardness-to-modulus ratio of a polymeric hard coating, as measured by nanoindentation, with the Taber† abrasion test.[6] These "Top" nanomechanical measurements can be compared directly with the "Top" FTIR-ATR spectroscopy scans.

In addition to the "Top" measurements, "Cross-section" quasi-static measurements were also performed on the coating samples by cutting sections from the plastic panels, mounting them in epoxy and polishing the cross-section faces. Indents were made in a straight line pattern at an approximate 10° angle to the coating surfaces to obtain mechanical data as a function of coating depth. Indents were performed with a five micron spacing and at roughly half the indentation depth used in the "Top" measurements. Five indent "lines" were performed for each sample condition. In some cases data from an indent line was unusable for analysis and the data from the entire line was discarded. All data reported represents results from three to five indent lines per sample. As with the FTIR-ATR testing, "Top" and "Cross-section" nanoindentation testing for a given coating type was performed at locations with the same coating thicknesses to ensure that top and bottom surface results would be directly comparable for a given coating regardless of lamp type used during cure.

Standard Physical Property Measurements

A replicate set of samples, cured with the same conditions as the samples described in this report, had been previously tested for standard surface cure physical properties: abrasion resistance and chemical resistance. In the case of abrasion resistance, testing was done with a Taber† abrasion tester (ASTM D1003/D1044). In this test a lower percent change in haze compared with an un-abraded sample signifies less abrasion damage to the surface. Surface chemical resistance was evaluated using an MEK soak test (ISO 12944). A cloth soaked with MEK was applied to the coating surface for 10 minutes and then the coating surface was wiped dry. The coating was rated with a score from "0" (no change in the surface quality) to "5" (total loss of coating adhesion.) Results from these tests are discussed in the context of the FTIR-ATR and nanomechancial data presented here. In the interest of space, figures and graphs detailing these results are not included in this report.

Results and Discussion

Three Year Weatherable Standard Coating (3YR-STD)

The "Top and "Bottom" FTIR-ATR results are shown in Figures 1 a, b and c for the 3YR-STD coating cured with the Hg, Fe, and Ga lamps, respectively. For each of the lamps, the "Top" spectroscopic data show a clear progression of higher percent cure with higher dose. The Hg and Ga lamps show very similar levels of conversion at each dose, whereas the Fe lamp shows a significantly lower level of conversion. The "Bottom" spectroscopic data also show a progression to higher cure levels at higher dose, although the total magnitude of difference between high and low dose is much smaller. Overall, in contrast to the "Top" measurements, the "Bottom" measurements show little difference between the 3YR-STD conversion curves for the three lamps studied. All FTIR-ATR measurements in this series were performed at locations where the hardcoat thickness was measured to

be approximately 9.9 microns. Standard physical property measurements of Taber† abrasion resistance and chemical resistance (to MEK solvent) show a similar trend of highest resistance for the 3YR-STD coating cured with the Hg-lamp, intermediate resistance when cured with the Ga-lamp, and the lowest resistance when cured with the Fe-lamp.

The absence of a difference in cure level for the "Bottom" scans suggests that at these coating thicknesses (nominally 10 microns), the intensity of light penetrating through the coatings is not a function of lamp type. The relative intensities of the UV-B and UV-C components of the three lamp spectra were compared after normalizing with the relative intensities of the UV-A components. This analysis showed that for UV-B the Hg and Ga lamps had similar levels and were about double that of the Fe-lamp. For UV-C the Hg lamp intensity was more than double that of the Ga lamp which in turn was double that of the Fe-lamp. The better the overlap of the absorption and excitation wavelengths, and the stronger the intensity of light at these points of overlap, the more efficient the cleavage of the photoinitiator and the higher the observed conversion level. Together, these results suggest that the Hg and Ga lamps are more efficient at initiating cure in the 3YR-STD system than the Fe lamp.

Interestingly, the Fe-lamp cured sample shows a higher overall level of cure at the "Bottom" location than the "Top" location. If the Fe-lamp is less efficient at initiating the cure reaction, this result may be explained by an increased likelihood for oxygen inhibition at the surface of these samples.[7] The interior cure would be unaffected by this but the top surface cure might be significantly reduced, resulting in a lower observed conversion level compared with the bottom surface.

Figure 1. Conversion as measured by FTIR-ATR for 3YR-STD as a function of exposure: (a) Hg-lamp, (b) Fe-lamp, (c) Ga-lamp.

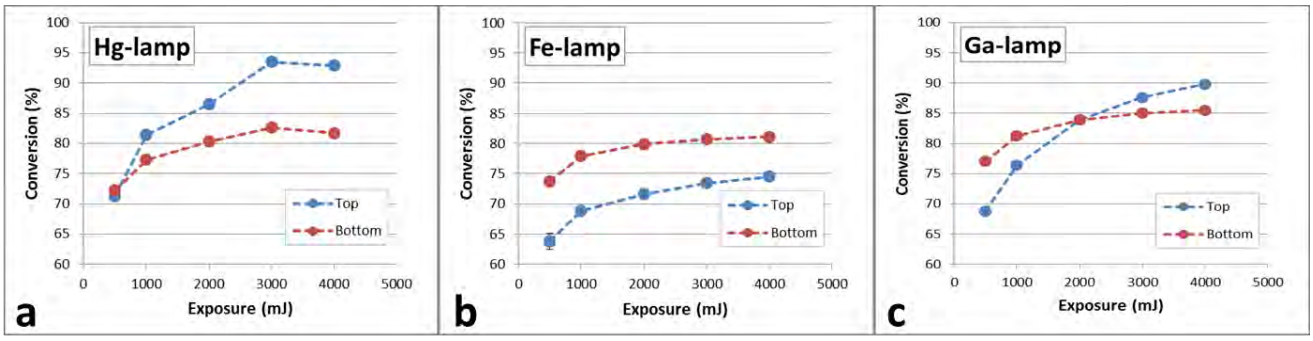

Note: Test data. Actual results may vary.

The "Top" nanomechanical testing results are shown in Figure 2 for the three lamps Hg, Fe, and Ga. The data in Figures 2 a, b and c represents the results for modulus, hardness, and H/E_r, respectively. The "Top" modulus data shows no clear trend with either dose or lamp type. In contrast, the abrasion resistance measures of hardness and H/E_r show clearer differences between the lamp types. Until about 3,000 mJ the samples cured with the Hg lamp show better performance. The other two lamps show a more steady increase in abrasion resistance as a function of exposure energy. The performance of the samples cured with the Ga lamp is predicted to be superior to those cured with the Fe lamp at exposure ranges above 500 mJ.

The abrasion resistance data is consistent with the "Top" results as measured by FTIR-ATR, with the performance of the 3YR-STD sample cured with the Hg-lamp slightly better than that of the same sample cured with the Ga-lamp and both significantly superior to a sample cured with the Fe-lamp. The modulus data does not show the same trend as seen in the hardness data. This may be explained by the greater variability in the modulus data for this sample or may indicate that the modulus value plateaus above a conversion of 65%. Alternatively, this may be explained by the nature of the modulus measurement. The zone of elasticity extends much deeper into the test sample during a modulus measurement compared with the zone of plasticity for the hardness measurement, so that the modulus measurement effectively samples a response deeper into the coating.[8] If this last explanation is correct it suggests that the bulk of the coating may have different properties from the immediate surface.

Figure 2. Nanomechanical properties measured for 3YR-STD "Top": (a) Modulus, (b) Hardness, (c) Hardness to Modulus Ratio.

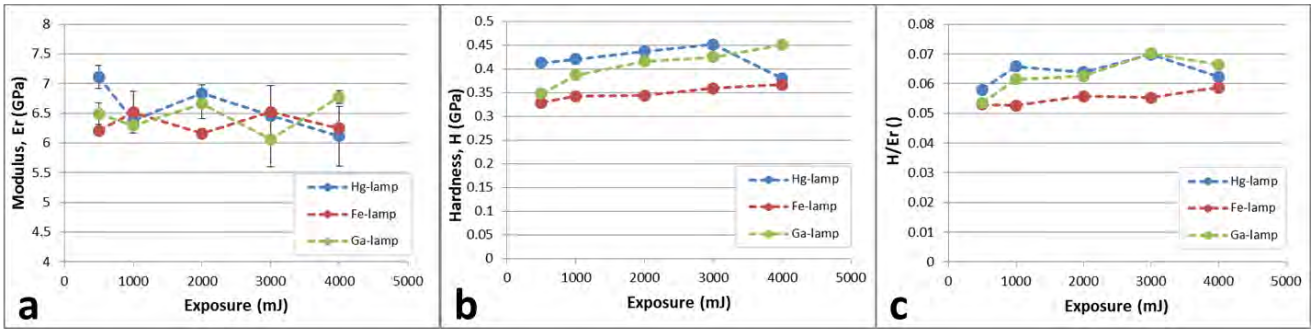

Note: Test data. Actual results may vary.

Cross-sectional nanoindentation was performed to determine the mechanical property differences as a function of coating depth for the different lamp types and exposure levels. Cross-sectional samples for this series were cut from locations where the hardcoat thickness was measured to be approximately 12.9 microns. Test depths shown in Table 1 were consistent between all measurements of this series.

Table 1. Contact test depths for cross-sectional nanoindentation measurements of the 3YR-STD series

	Hg 500 mJ	Hg 4,000 mJ	Fe 500 mJ	Fe 4,000 mJ	Ga 500 mJ	Ga 4,000 mJ
Average (nm)	331	331	335	345	331	328
Stdev (nm)	2	2	4	5	7	2
Difference (nm)	0		10		3	

Note: Test data. Actual results may vary.

The true distance from the epoxy/hardcoat interface was calculated in each case using the known distance of travel in the x-axis of each indent in the line and the true angle of the indent line to the interface. Indents were visible across each layer (epoxy, hardcoat, and polycarbonate) using the nanoindenter optics, making this calculation possible. Using the interface locations identified optically, the results for modulus and hardness of the hardcoat between the two interfaces were plotted. The results are shown for the Hg, Fe, and Ga lamps in Figures 3 a, b and c.

A key observation from the "Cross-section" data is the fact that there is very little evident change in modulus or hardness as a function of depth from the top surface (at the interface with the epoxy) to the bottom surface (at the interface with the polycarbonate.) These results indicate that the bulk of the hardcoat behaves similarly to the bottom surface, suggesting a very steep change from the surface to the bulk properties at the top interface. Additionally, the modulus and hardness values for samples cured with each of the three lamps are remarkably consistent with each other. In the case of the Hg and Ga lamps, it is noted that the modulus and hardness values for the lowest dose samples (500 mJ) are directionally higher than the highest dose samples (4,000 mJ). However, the spread of the data is such that the 95% confidence intervals for these datasets (not shown) overlap and the shift observed is not actually statistically significant. It is also observed that the Fe-lamp cured samples show a slight drop in hardness at the locations closest to the epoxy/hardcoat interface. This may signify a slightly lower value of hardness at the very top surface of the sample compared with the bulk. This result is consistent with the "Top" nanoindentation measurements which showed that the Fe-lamp cured samples had the lowest hardness of the series.

Figure 3. Cross-sectional nanoindentation results for 3YR-STD: (a) Hg-lamp (b) Fe-lamp (c) Ga-lamp.

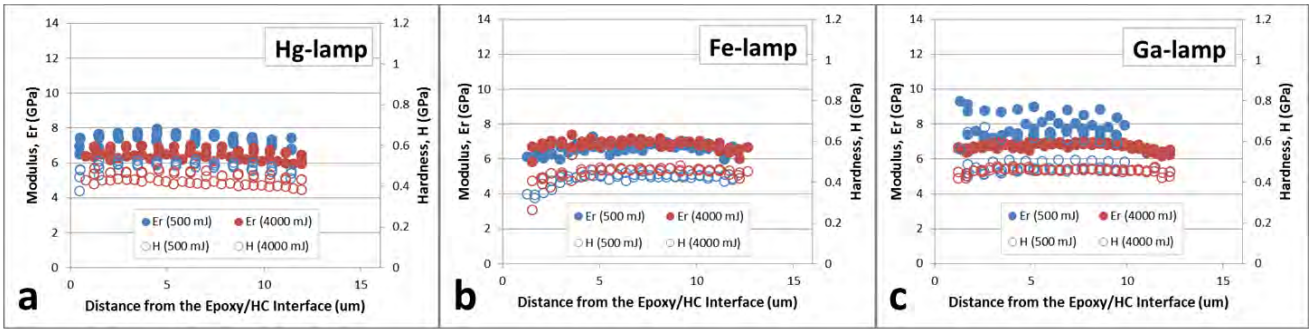

Note: Test data. Actual results may vary.

Five Year Weatherable Standard Coating (5YR-STD)

The FTIR-ATR results for the five year weatherable coating are shown in Figure 4 for the three different lamps and the five different exposure energies tested. All FTIR-ATR measurements in this series were performed at locations where the hardcoat thickness was approximately 7.5 microns. As with the 3YR-STD data (Figure 1), the "Top" data for all three lamp types shows a steady progression to higher levels of conversion with higher exposure energy. Also in agreement with the 3YR-STD data, the highest conversion is obtained for the Hg-lamp cure, followed closely by the Ga-lamp, with significantly lower levels of conversion observed in the case of the Fe-lamp. As discussed, these results could be explained by the observation that the Ga-lamp has a spectrum with UV-B and UV-C intensity levels close to those of the Hg-lamp whereas the intensity levels of the Fe-lamp are significantly lower in both UV-B and UV-C. The standard physical property Taber† abrasion shows a much higher resistance for the 5YR-STD coating cured with the Hg lamp compared to the Ga and the Fe lamps. Testing of chemical resistance (to MEK solvent) shows higher resistance for the 5YR-STD coating cured with the Hg-lamp than with the Ga-lamp, and the lowest resistance when cured with the Fe-lamp.

As was also observed in the 3YR-STD system, the "Bottom" curves are measured to all have roughly the same level of conversion as a function of exposure, regardless of lamp type. As discussed,

this result would be consistent with the interpretation that sufficient light intensity reaches through these relatively thin coatings such that the differences in the lamp spectra are not observed at the maximum coating depth of about 10 microns used in these assemblies.

Finally, the Fe-lamp data is notable in that it shows the same reversal in cure level as was seen in the 3YR-STD measurements: the "Bottom" conversion dataset is higher than that of the "Top" dataset. As discussed, this is likely caused by higher levels of oxygen inhibition at the top surface of this sample due to poorer efficiency of double bond conversion compared with the Hg and Ga-lamps.

Figure 4. Conversion as measured by FTIR-ATR for 5YR-STD as a function of exposure: (a) Hg-lamp, (b) Fe-lamp, (c) Ga-lamp.

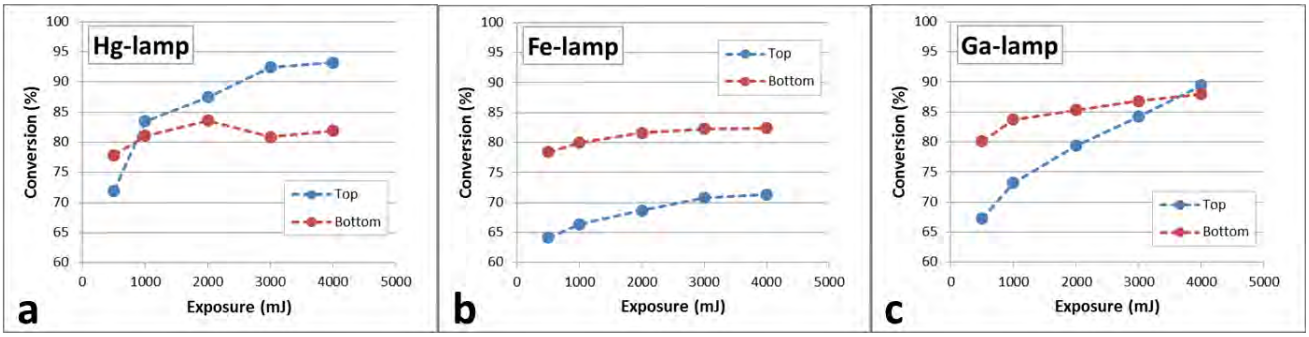

Note: Test data. Actual results may vary.

The nanomechanical results for the "Top" measurements are summarized in Figure 5. For each of the three measures examined, modulus (Figure 5a), hardness (Figure 5b) and H/E_r (Figure 5c), the trends with lamp type and exposure are consistent. Samples cured with the Hg lamp have the highest modulus at exposure levels above 3,000 mJ. At all exposure levels, the abrasion resistances of samples cured with the Hg lamp, as measured by hardness and the ratio H/E_r are predicted to be higher than samples cured with the other lamps. The mechanical properties of the samples cured with the Fe lamp are consistently lowest in performance, while the samples cured with the Ga lamp are intermediate in performance. These trends are very similar to what was observed for the 3YR-STD samples, although the differences between lamp type are greater in the the 5YR-STD coatings.

Figure 5. Nanomechanical properties measured for 5YR-STD "Top": (a) Modulus, (b) Hardness, (c) Hardness to Modulus Ratio

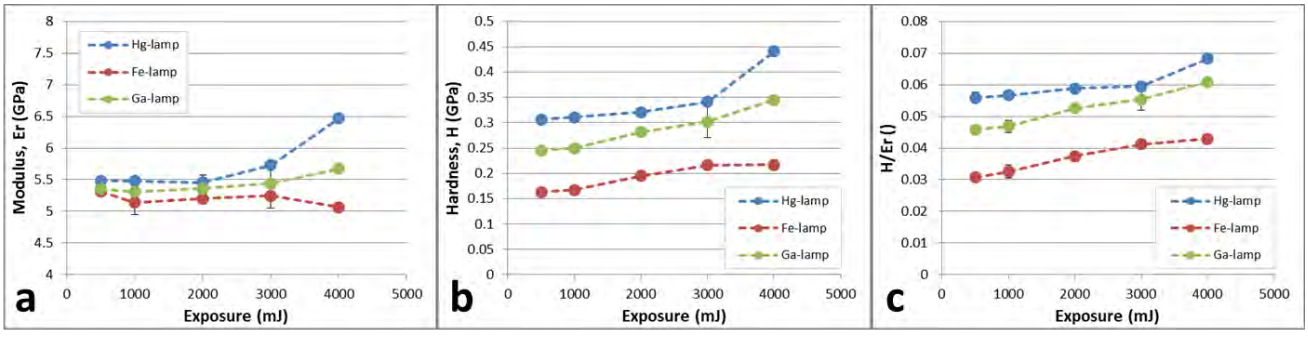

Note: Test data. Actual results may vary.

In comparison with the 3YR-STD results, the modulus and hardness values for the 5YR-STD samples are slightly lower for each lamp type. This is consistent with the formulation changes for these two grades. The 5YR-STD coating was formulated to preference long weatherability over high abrasion resistance. The formulation changes are expected to reduce both the modulus and the hardness of the coating. Comparative standard physical property measurements of abrasion and solvent resistance resistance showed that the 3YR-STD coating has higher resistance compared with 5YR-STD coating when cured with all three lamp types, a result consistent with these findings.

As with the 3YR-STD coatings, the 5YR-STD coatings were potted and polished in cross-section to enable a study of the nanomechanical properties as a function of coating depth (Figure 6.) Cross-sectional samples for this series were cut from locations where the hardcoat thickness was measured to be approximately 9.0 microns. The test depths were very consistent for the Fe and Ga lamp cured samples of this series, as shown in Table 2. However, some deviation was observed between the test depths for the two Hg lamp cured samples studied (500 mJ and 4,000 mJ.) The difference in the two sets of data (12 nanometers) is small but significant given the low variability of each individual dataset. It is possible this difference in test depth could explain the higher hardness values for the 4,000 mJ Hg-lamp data of Figure 6; a lower test depth in nanoindentation does typically result in a higher value of hardness and modulus. However, is noted that a comparable shift was not observed in the modulus data.

Figure 6. Cross-sectional nanoindentation results for 5YR-STD: (a) Hg-lamp (b) Fe-lamp (c) Ga-lamp.

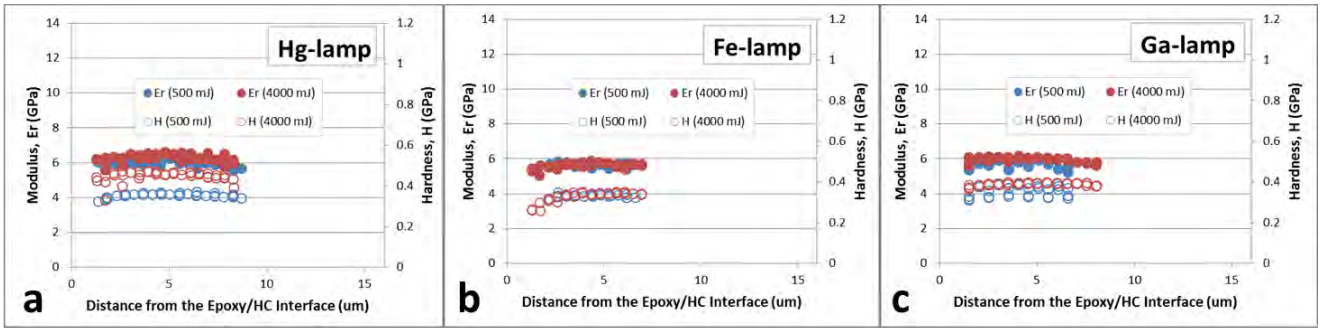

Note: Test data. Actual results may vary.

Table 2. Contact test depths for cross-sectional nanoindentation measurements of the 5YR-STD series.

	Hg 500 mJ	Hg 4,000 mJ	Fe 500 mJ	Fe 4,000 mJ	Ga 500 mJ	Ga 4,000 mJ
Average (nm)	339	327	339	341	335	331
Stdev (nm)	2	3	2	5	4	2
Difference (nm)	12		3		4	

Note: Test data. Actual results may vary.

As with the 3YR-STD coatings, the most important observations about the cross-sectional results in Figure 6 are that there is generally little change in modulus or hardness as a function of depth or dose or lamp type. The intensity of all three lamps was sufficient to achieve a consistent level of cure throughout these coatings, likely due to the fact that the coating layer is thin and unpigmented. A slight

decrease in hardness is again observable in the Fe-lamp system at the location closest to the epoxy/hardcoat interface. This is the sample which also had the lowest hardness value in the "Top" nanoindentation testing. Compared to the modulus and hardness values for the 3YR-STD coating system (Figure 3), the values of the 5YR-STD system shown here are slightly lower. As discussed, the formulation changes between these coatings would reasonably result in a lower modulus and hardness.

Three Year Weatherable Modified Coating (3YR-MOD)

Figure 7 compares the percent conversion results as measured by FTIR-ATR at the top and bottom coating surfaces for the 3YR-MOD series. All FTIR-ATR measurements in this series were performed at locations where the hardcoat thickness was measured to be approximately 10.1 microns. As with the other two coatings studied, the "Top" results show the highest conversion for the Hg-lamp with intermediate conversion for the Ga-lamp and the lowest conversion for the Fe-lamp. Additionally, all of the "Top" datasets for this coating show increasing conversion with increased dose. Consistent with the FTIR-ATR data, the standard physical property measurements of Taber† abrasion resistance and chemical resistance (to MEK solvent) also show the highest resistance for the 3YR-MOD coating cured with the Hg-lamp and the lowest resistance when cured with the Fe-lamp.

Figure 7. Conversion as measured by FTIR-ATR for 3YR-MOD as a function of exposure: (a) Hg-lamp, (b) Fe-lamp, (c) Ga-lamp.

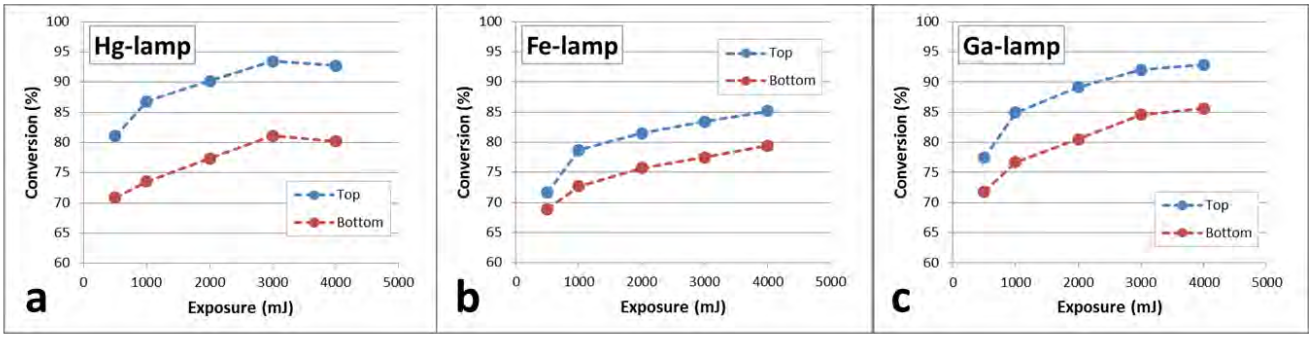

Note: Test data. Actual results may vary.

In contrast to the results for the other two coatings studied, in this case the "Bottom" conversion levels for the Fe-lamp series are all below those of the "Top" conversion levels. As was discussed in the Sample Preparation section, the formulation for the 3YR-MOD coatings was modified compared to the 3YR-STD coating to achieve higher double-bond conversion at the same energy dose level. The results here are consistent with this type of formulation change. In the 3YR-STD coating it was hypothesized that the lower conversion for the "Top" of the Fe-lamp cured samples was due to a slower cure initiation at the top surface due to a relatively lower intensity UV-B and UV-C spectrum compared with the other lamps. A slower cure was expected to enable more oxygen inhibition, resulting in an ultimately lower top surface cure. By enabling higher double-bond conversion at the same energy dose level, the 3YR-MOD coating appears to have resolved this issue. In the case of the Fe-lamp, the lower intensity UV-B and UV-C bands are now able to initiate cure at a rate that no longer appears to bias oxygen inhibition reactions at the surface of this 3YR-MOD coating formulation.

The conversion level of the "Top" and "Bottom" locations for the other lamps is only slightly improved (about 8% higher) at the lowest dose level for the 3YR-MOD coatings compared with the 3YR-STD coatings. The most significant change in conversion was observed for the Fe-lamp, as discussed.

In comparison with the 3YR-STD and 5YR-STD coatings, the 3YR-MOD coatings in Figure 8 showed the smallest different between the modulus, hardness and H/E_r values for the different lamps. Specifically, the Fe-lamp cured samples showed an overlap in properties with those cured using the other two lamps, even at lower exposures. These results suggest that the changes made in the 3YR-MOD coating to increase the sensitivity of the coating to UV dose has virtually eliminated the physical property differences at the surface of the samples. A comparison of the magnitude of the three properties shown in Figure 8 with those of Figure 2 does not otherwise show a large shift to higher values for the Hg and Ga lamps. The main effect appears to be in the top surface nanomechanical data for samples cured with the Fe-lamp.

Figure 8. Nanomechanical properties measured for 3YR-MOD "Top": (a) Modulus, (b) Hardness, (c) Hardness to Modulus Ratio

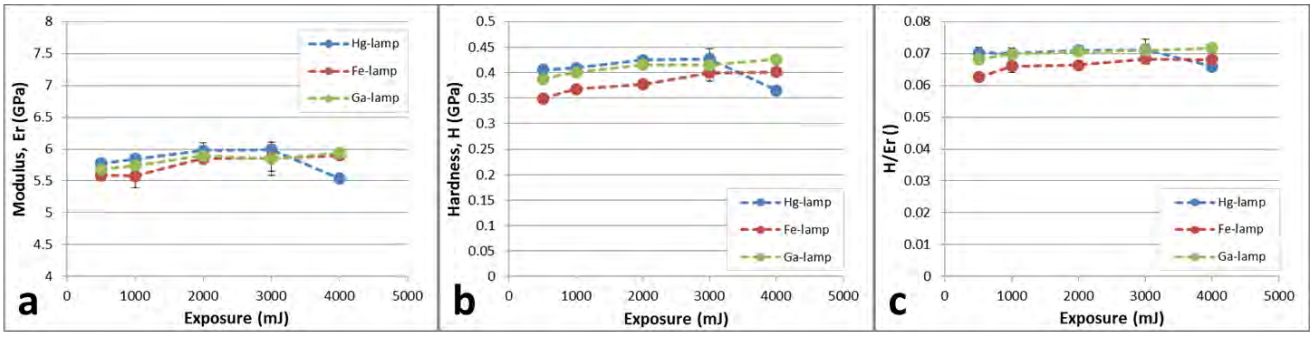

Note: Test data. Actual results may vary.

Cross-sectional samples for this series were cut from locations where the hardcoat thickness was measured to be approximately 13.1 microns and results are shown in Figure 9 for the 4,000 mJ exposure. Cross-sectional data at 500 mJ was not available for these samples. Although all sample sets in this paper were cross-sectioned and polished following equivalent procedures, the 3YR-MOD 500 mJ cure samples displayed a height difference for the hardcoat layer compared with that of the epoxy and polycarbonate layers that prevented the imaging of the indent lines and the identification of the interface locations. The fact that the same polishing procedure resulted in a height difference of the hardcoat layer suggests there may be a difference in mechanical properties for the 3YR-MOD 500 mJ samples compared with the 3YR-MOD 4,000 mJ samples. However in looking at the "Top" and "Bottom" FTIR-ATR data (Figure 7), the change in conversion is within the same order of magnitude as for the 3YR-STD samples (Figure 1.) Likewise, there is little change in "Top" nanoindentation properties as a function of exposure (Figure 8) or compared with the 3YR-STD samples (Figure 2.)

Compared with the cross-sectional nanoindentation results for the other two series, the 3YR-MOD samples at 4,000 mJ showed some interesting differences in gradient and magnitude. The modulus and hardness show higher values at the epoxy/hardcoat interface (the top of the hardcoat layer) and lower values at the polycarbonate/hardcoat interface (the bottom of the hardcoat layer.) This effect

is most pronounced for the Fe and Ga-lamp cured samples. At the bottom of the hardcoat, the modulus and hardness values are consistent with the values obtained for the 3YR-STD samples (about 6 GPa and 0.4 GPa, respectively); however, at the top of the hardcoat the values are much higher, particularly for the Fe and Ga-lamp cured samples. These results are consistent with the formulation change for the 3YR-MOD samples that was made to increase UV sensitivity. That the observed changes in physical properties are so much greater when tested in cross-section compared with top-down measurements of FTIR-ATR and nanoindentation is not surprising because these techniques yield results averaged over a sampling depth. When testing in a cross-section configuration there is no change in material properties as a function of sampling depth. In contrast, when testing in a top-down configuration a higher value at the very top surface will be depressed by lower values immediately below that surface.

Figure 9. Cross-sectional nanoindentation results for 3YR-MOD: (a) Hg-lamp (b) Fe-lamp (c) Ga-lamp.

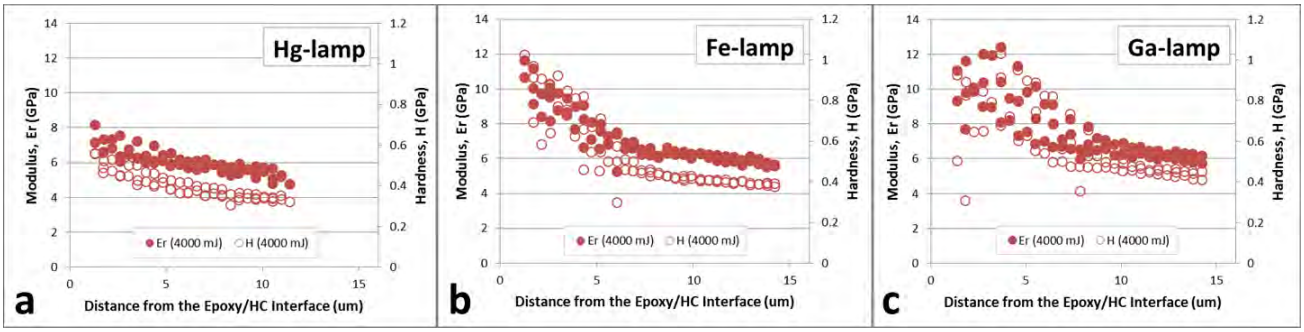

Note: Test data. Actual results may vary.

Summary and Conclusions

For the two standard coating types studied (3YR-STD and 5YR-STD), the top surface properties show a consistent trend of higher conversion and better standard physical and nanomechanical properties for samples cured with the Hg-lamp compared to the Ga-lamp. Samples cured with the Fe-lamp consistently had the lowest conversion, standard physical and nanomechanical properties when measured at the top surface. The details of the UV spectra for each lamp, normalized on UV-A intensity were provided as a rationale for this result: the UV-B intensities for the three lamps follow the trend Hg ~ Ga > Fe, and the UV-C intensities for the lamps follow the trend Hg > Ga >> Fe. Formulation modifications of the 3YR-MOD coating improved properties most notably for samples cured by the Fe lamp.

By FTIR-ATR, the bottom surface conversion is roughly the same for all three lamps and all three coatings. Since the coatings are relatively thin (nominally 10 microns) and formulated without pigment, this result is perhaps not that surprising. The conclusion must be that the intensity of light penetrating from top to bottom is not significantly different for the different lamps. In the absence of inhibition from oxygen (as is present at the top surface) all coatings cure to the same extent regardless of lamp type. Oxygen inhibition, a surface phenomenon, appears to be an important factor for both UV lamp type and coating type. In the standard coatings (3YR-STD and 5YR-STD) the conversion and physical properties were depressed for the top surface of samples cured with the Fe-lamp, a lamp with a known lower intensity in UV-B and UV-C. A change in formulation (3YR-MOD) to improve the sensitivity to UV dose resulted in a coating with improved top surface conversion and mechanical

properties when cured by the Fe-lamp. By increasing the sensitivity to the dose, the effects of oxygen inhibition appear to be suppressed in the 3YR-MOD coating compared with the 3YR-STD coating. It would be of interest in a future study to repeat this experiment in an inert atmosphere to validate this hypothesis.

By cross-section nanoindentation, there is no obvious gradient (slope) in modulus or hardness from the top surface of the hardcoat (the epoxy/hardcoat interface) to the bottom surface of the hardcoat (the hardcoat/polycarbonate interface) for the two standard coatings. These results indicate that the bulk of the hardcoat behaves similarly to the bottom surface. In contrast, the 3YR-MOD coating displayed significant gradients in cross-section testing.

Taken together, the results from this analysis show the value of nano-mechanical measurements when used in concert with spectroscopic data and standard physical property techniques. There are important cure differences to understand between the different coating types and their interactions with the various lamps and as a function of hardcoat depth.

Acknowledgements

The authors gratefully acknowledge the help of the following individuals at Momentive Performance Materials in the execution of this work: Thomas Kaupat (sample preparation), Dr. Sarah Lewis (FTIR-ATR), and James Pawlson (nanoindentation.)

† Power Puck and EIT are trademarks of Electronic Instrumentation & Technology Inc.
† Nicolet and Smart Orbit are trademarks of Thermo Fisher Scientific Inc.
† TriboIndenter is a trademark of Hysitron, Inc.
† Taber is a trademark of Taber Industries.

References

1. Gu, X.; Michaels, C.A.; Drzal, P.L.; Jasmin, J.; Martin, D.; Nguyen, T.; Martin, J.W., "Probing photodegradation beneath the surface: a depth-profiling study of UV-degraded polymeric coatings with microchemical imaging and nanoindentation." J. Coat. Technol. Res., 4 (4), 389-399 (2007).
2. Cordelle, A.; Drissi-Habti, M., "Nanoindentation characterization of vinylester glass-fiber composites submitted to dense ultraviolet radiation exposure." Mater. Eval., 4 (71), 466-473 (2013).
3. Forster, A.M.; Michaels, C.A.; Sung, L.; Lucas, J., "Modulus and chemical mapping of multilayer coatings." ACS Appl. Mater. Inter., 1 (3), 597-603 (2009).
4. Hall, C.J.; Murphy, P.J.; Griesser, H.J., "Direct imaging of mechanical and chemical gradients across the thickness of graded organosilicone microwave PECVD coatings." ACS Appl. Mater. Inter., 6, 1279-1287 (2014).
5. Leyland, A.; Matthews, A., "On the significance of the H/E ratio in wear control: a nanocomposite coating approach to optimized tribological behavior." Wear, 246, 1-11 (2000).
6. David, J.; Hayes, R.; Hui, J.; Nay, R., "Nanoindentation as an alternative to mechanical abrasion for assessing wear of polymeric automotive coatings." J. Coat. Technol. Res., *in press*.
7. Ligon, S.C.; Husar, B.; Wutzel, H.; Holman, R.; Liska, R., "Strategies to reduce oxygen inhibition in photoinduced polymerization." Chem. Rev., 114, 557-589 (2014).
8. Beake, B.D.; Goodes, S.R.; Smith, J.F.; Fox-Rabinovich, G.S.; Veldhuis, S.C. (2010). Using nanomechanics to optimize coatings for cutting tools. In S. Zhang (Ed.), *Handbook of Thin Films and Coatings: Nanostructured Thin Films and Coatings – Mechanical Properties, Vol.1* (pp. 205-244) Boca Raton, FL: CRC Press.